Microwave and THz sensing using slab-pair-based metamaterials

G. Kenanakis [a,b,*], N.-H. Shen [a,c], Ch. Mavidis [a,d], N. Katsarakis [a,b], M. Kafesaki [a,e], C.M. Soukoulis [a,c], E.N. Economou [a]

[a] Institute of Electronic Structure and Laser, Foundation for Research and Technology—Hellas, P.O. Box 1385, Vassilika Vouton, 711 10 Heraklion, Crete, Greece
[b] Science Department, School of Applied Technology, Technological Educational Institute of Crete, 710 04 Heraklion, Crete, Greece
[c] Ames Laboratory—USDOE, and Department of Physics and Astronomy, Iowa State University, Ames, IA 50011 USA
[d] Department of Electrical Engineering, Stanford University, Stanford, CA 94395, USA
[e] Department of Materials Science and Technology, University of Crete, 710 03 Heraklion, Crete, Greece

ARTICLE INFO

ABSTRACT

In this work the sensing capability of an artificial magnetic metamaterial based on pairs of metal slabs is demonstrated, both theoretically and experimentally, in the microwave regime. The demonstration is based on transmission measurements and simulations monitoring the shift of the magnetic resonance frequency as one changes a thin dielectric layer placed between the slabs of the pairs. Strong dependence of the magnetic resonance frequency on both the permittivity and the thickness of the dielectric layer under detection was observed. The sensitivity to the dielectrics' permittivity (ε) is larger for dielectrics of low ε values, which makes the approach suitable for sensing organic materials also in the THz regime. The capability of our approach for THz sensing is also demonstrated through simulations.

© 2012 Elsevier B.V. All rights reserved.

1. Introduction

Metamaterials have attracted intense research attention in recent years, due to their unique response to electromagnetic radiation and the possibility of engineering their electromagnetic properties to a much greater extent than what is possible in natural materials, and to achieve unusual and unique properties, such as optical magnetism, negative index of refraction [1] etc., enabling many unique applications, like perfect lensing [2], invisibility cloaks [2,3], etc.

Sensing could be listed as one of the areas where metamaterials offer revolutionary advancements, as stated in Refs. [4,5]. It has been proposed that metamaterials can be used in microwaves, e.g. for evaluation of dielectric materials [6], in the visible region, e.g. for the detection of biomolecules [7,8], and the measurement of gas concentrations [9,10], as well as in the monitoring of chemical reactions [11].

Microwaves are frequently used in sensing applications, e.g. in medical and aerospace industries, offering over traditional sensors many advantages, such as rapid, nondestructive, precise, and fully automated measurement which can be made in a laboratory or online. They permit relatively high spatial resolutions compared to other techniques and they do not require physical contact with the processed material, and still respond to the presence or absence of an object of interest [6]. Furthermore, microwave sensing techniques are relatively inexpensive and do not require extensive data analysis [6].

One of the most common metamaterial elements which has been widely demonstrated in microwaves is the split ring resonator (SRR), which was first proposed in 1999 [12]. SRR consists of a metallic ring with a split (or more than one co-centric rings with splits) on a dielectric substrate. The loop-like currents in the ring (excited by an incident EM wave) make it act as an inductor, while the split, where opposite charges are accumulated, acts as a capacitor [13–14], making the system behave as an effective inductor–capacitor (LC) circuit, showing a resonant electromagnetic response at a frequency $\omega_\mu = 1/\sqrt{LC}$. SRR has been extensively studied for its sensing capabilities in microwaves; it has been observed to have a significant sensing feature for different kinds of materials, such as bioassays [15], photoresist AZ9260 [16], liquids and their contaminations [17].

In each of the above cases, the capacitance of the SRR structures is changed by adding the substance of interest to the SRR, mainly in the SRR split/splits, giving a shift to the resonant frequency, detectable in simple transmission measurements. However, since a significant amount of electric field at the SRR split is located in the substrate [18], the capacitance of the structure cannot be highly affected by the substance under detection and it is mainly affected by the permittivity of the

* Corresponding author at: Foundation for Research and Technology—Hellas (FORTH), Institute of Electronic Structure and Laser (IESL), P.O. Box 1385, Vassilika Vouton, 711 10 Heraklion, Crete, Greece. Tel.: +30 2810391917; fax: +30 2810391951.
E-mail address: gkenanak@iesl.forth.gr (G. Kenanakis).

substrate dielectrics [18]. In terms of practical applications, this limits the utility of the SRR as a sensing device [19].

An alternative metamaterial structure that seems to be more suitable for microwave and THz sensing applications is a pair of slabs (see Fig. 1) [20], which, similar to the SRR, exhibits a resonant magnetic response (resonant magnetic moment) coming from loop-like currents. The structure has certain advantages over the SRR, due to its simplicity in fabrication and the ability to exhibit a resonant and negative permeability response for incidence normal to the plane of the pairs, and thus using just a monolayer of slab pairs.

The advantage of the slab-pair structure over the SRR regarding sensing applications is based on the fact that for relatively wide slabs (see Fig. 1) the electric field at the capacitive areas of the structure is entirely confined between the slabs and thus it is very strongly affected by the permittivity of the material located between the slabs. This property, combined with the easiness in the fabrication and handling of microwave (mm-size) slabs, and thus the possibility to easily insert various materials between the slabs, offers a great approach to accurately evaluate the electrical permittivity of the material between the slabs and thus to detect small changes in this permittivity.

In this work we use the above mentioned approach to demonstrate (both theoretically and experimentally) the sensing capability of slab-pair systems. Inserting various dielectric materials between the slabs of the pair, we show that one can accurately estimate the permittivity of those materials, detecting even very small changes in this permittivity, ε. Our current experimental data concern structures operating in the frequency range 7–16 GHz; the sensing approach and structures though (with proper scaling), as shown by simulations, can be applied equally well in far infrared and THz regimes, with only limitations being the ones stemming from the practical realization of the device.

2. Experimental data and numerical simulations

The slab-pair structures employed in the present study are made of square slabs (see Fig. 1), offering the advantage of isotropy in the E–H plane, and thus of insensitivity on the incident wave polarization. The slabs are assembled as shown in Fig. 1;

each face (side) of the pair is printed (using a conventional printed circuit board process with 30 μm-thick copper patterns on FR-4 boards) on a separate thin board (of thickness $t_{\mathrm{b}}=0.6$ mm—see yellow color in Fig. 1—relative permittivity $\varepsilon_{\mathrm{b}}\sim3.8$ and dissipation factor $\tan\delta\sim0.025$ at 10.0 GHz). After their fabrication, two FR-4 boards bearing the metallic elements are placed facing each other, at a distance d, with the printed metallic structures facing outwards. The space of thickness d between the two FR-4 boards is filled (or partially filled) with the materials of interest (blue color in Fig. 1).

The total experimental sample possesses 10×10 unit cells (u.c.) in the plane coinciding with the directions of both the external electric and the magnetic fields. The distance d between the boards (equal to the thickness available for the material under sensing) varies between 0.5 and 1.5 mm.

The dielectric materials used in the experiments to test the sensing capability of our metamaterial structure are air, low density polyethylene (LDPE; Goodfellow Cambridge Ltd.), FR-4 and p-type silicon substrates (Silchem Handelsgesellschaft mbH). The dielectric properties of these materials are listed in Table 1, 2nd column.

The sensing capability of our metamaterial is studied using transmission measurements and corresponding simulations. The transmission measurements have been performed in free space, using a Hewlett-Packard 8722 ES vector network analyzer and microwave standard-gain horn antennas. For the transmission simulations we used a commercial three-dimensional full-wave solver (CST Microwave Studio) based on the Finite Integration Technique. We calculated the transmission considering an incident plane wave (with E, H, k as shown in Fig. 1) propagating through the system; the system has been considered as infinite along the E and H directions using periodic boundary conditions at the relevant boundaries.

3. Results and discussion

As has been already reported [21,22], the electromagnetic properties of slab pair metamaterials can be explained using equivalent inductor–capacitor (LC) circuits. For wide slabs (large w) as in our case (see Fig. 1), the inductance of the system can be approximately calculated in a similar way as in a solenoid, given by

$$L \approx \frac{\mu_0 l(d+2t_{\mathrm{b}})}{w} \tag{1}$$

where l and w are the length and the width of the slabs, respectively (in our case $l=w$), and $d+2t_{\mathrm{b}}$ is the thickness of the regime between the two metal elements of the pair (see Fig. 1; the permeability of both layers is assumed to be μ_0).

Fig. 1. Schematic of the slab-pair's structure. A magnification of one unit cell of the slab-pair's structure (red shadowed area) is presented. E, H, and k correspond to electric field, magnetic field, and wave vector, respectively. a_E and a_H (=9.5 mm) are the size of the unit cell along E and H directions, respectively. l=7 mm and w=7 mm are the length and the width of the metallic slabs (gray color), respectively, while d corresponds to the thickness of the materials of interest (blue color), placed between the two FR-4 boards (yellow color). (For interpretation of the references to colour in this figure legend, the reader is referred to the web version of this article.)

Table 1

Dielectric materials used for sensing, with their permittivities ε_x. The table lists the magnetic resonance frequency obtained by simulation, experiment, and using the last formula of Eq. (4).

Material (0.5 mm)	ε_x	Magn. resonant frequency (GHz)		
		Simulation	Experiment	[a]Eq. (4)
Air	1.00	14.17	14.22	Used for A_1, B_1
LDPE	2.28	11.88	11.88	11.867
FR-4	3.80	11.05	11.07	Used for A_1, B_1
Silicon	11.90	10.38	10.40	10.148

[a] For the evaluation of the coefficients A_1 and B_1 of Eq. (4) the materials used are air and FR-4.

Furthermore, the total capacitance C of the slab-pair structure can be approximated with that of two, in-series connected, parallel plate capacitors of relevant lengths $c_1 l$, w, and $(d+2t_b)$ along the E, H and k directions (see Fig. 1), respectively (c_1 is a numerical factor in the range $1/4 \leq c_1 \leq 1/5$, as can be concluded from electric field plots); thus C can be written as

$$C \approx \varepsilon_0 \varepsilon_{\text{eff}} \frac{w c_1 l}{2(d+2t_b)} \qquad (2)$$

In Eq. (2) ε_0 is the free-space permittivity and ε_{eff} is the relative permittivity of the material between the slabs, which in our case is the effective relative permittivity of the layered system formed by the dielectric boards supporting the metallic slabs, the material under sensing, and air (if the material under sensing does not fill all the space between the metallic elements of the pair). This permittivity can be calculated as [23]

$$\varepsilon_{\text{eff}} = \left(\sum_{m=1}^{n} \frac{d_m}{\varepsilon_m d_{\text{tot}}} \right)^{-1} = \left[\frac{1}{d_{\text{tot}}} \left(2\frac{t_b}{\varepsilon_b} + \frac{d-d_x}{\varepsilon_{\text{air}}} + \frac{d_x}{\varepsilon_x} \right) \right]^{-1} \qquad (3)$$

where ε_m, and d_m are respectively the relative permittivity and the thickness of each layer of the layered material, and d_{tot} is the total distance between the metal slabs. In our case, where the slabs are printed on FR-4 boards of thickness $t_b = 0.6$ mm, d_x is the thickness of the material of interest and ε_x its relative permittivity.

Taking into account the above equations, one can obtain the magnetic-resonance frequency of the system as

$$f_\mu = \frac{\omega_\mu}{2\pi} = \frac{1}{2\pi\sqrt{LC}} = \frac{1}{\sqrt{2c_1}\pi} \frac{c}{l} \frac{1}{\sqrt{\varepsilon_{\text{eff}}}} = \frac{A}{\sqrt{\varepsilon_{\text{eff}}}} = \sqrt{A_1 + \frac{B_1}{\varepsilon_x}} \qquad (4)$$

where c is the free space light velocity, $A = c/\pi l\sqrt{2c_1}$, while the constants A_1 and B_1 include the geometry and material parameters which do not depend on ε_x.

From Eq. (4) one can notice that the magnetic-resonance frequency of the slab-pair design is strongly dependent on the dielectric properties of the material between the slabs, especially if this material is of low permittivity value, lower than the permittivity of the FR-4 boards where the metal slabs are printed. This sensitivity is confirmed by the detailed experimental and numerical data presented in Fig. 2.

Fig. 2 shows the simulation (upper panel; solid lines) and experimental results (lower panel; dotted lines) regarding the transmission coefficient of the four materials listed in Table 1, for thickness $d=d_x=0.5$ mm. Aside from the very good agreement between simulations and experiments, one can observe in Fig. 2 a quite large shift of the magnetic resonance to lower frequencies as the permittivity of the dielectric between the slab-pairs changes from 1.0 (air) to 11.90 (silicon). The relative shift is larger for materials of lower permittivity, as suggested by Eq. (4).
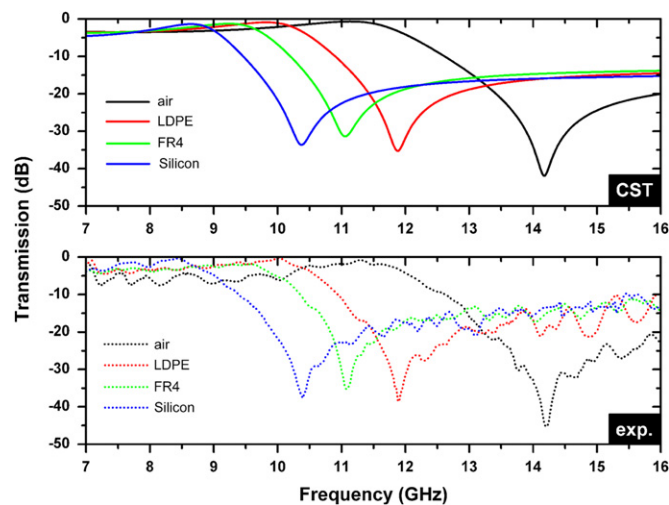
Indeed, the last expression in Eq. (4) can be used for a quite accurate evaluation of the electrical permittivity of the material between the slabs if the values of the constants A_1 and B_1 for each geometric configuration are available (these values can be calculated by considering the transmission for two known materials). For the configuration of Fig. 2 and using the calculation of A_1 and B_1 the magnetic resonance frequency for air ($f_{\mu,\text{air}} = 14.17$ GHz) and FR-4 ($f_{\mu,\text{FR-4}} = 11.05$ GHz), one can find $A_1 = 94.00$ GHz^2 and $B_1 = 106.789$ GHz^2. For this choice of A_1 and B_1, the last expression of Eq. (4) can reproduce very well the numerical and experimental f_μ vs ε_x data, especially for materials of low permittivity values (lower than that of the dielectric (FR-4) board on which the metallic pair is printed), as shown in Fig. 3 and indicated also by column 5 of Table 1.

Besides the quantitative power of the last expression in Eq. (4), the preceding relation $f_\mu = A/\sqrt{\varepsilon_{\text{eff}}}$ of Eq. (4) in combination with Eq. (3) offers a nice qualitative expression of the magnetic resonance frequency dependence on ε_x, which can be used to optimize the sensing design. These equations suggest that an easy way to enlarge the sensitivity of our design and to achieve high sensitivity in a broader permittivity ε_x range is to print the slabs on higher-index dielectrics (i.e. of larger ε_b), since ε_{eff} is more strongly influenced by the lower-index material of the layered structure. Indeed, for slabs of the same geometrical features as those of Fig. 2 but printed on silicon boards ($\varepsilon_b = 11.9$), the sensitivity of the structure becomes larger than that shown in Fig. 2 and is maintained for materials of higher ε_x, as shown by related simulations (not shown here). For example the difference $\Delta f = f_\mu(\varepsilon_x=6) - f_\mu(\varepsilon_x=5)$ which for the FR-4 board case is 0.15 GHz becomes ~ 0.25 GHz for the Si case.

As Eqs. (3) and (4) suggest, the magnetic resonance frequency of our structure will depend also on the thickness of the material under sensing. This dependence is examined in Figs. 4 and 5.

Fig. 4 shows the simulated transmission as a function of frequency for the geometry of Fig. 2, but for the space between the slabs (of thickness $d=0.5$ mm) only partially filled with LDPE;

Fig. 2. Simulation (upper panel; solid lines) and experimental results (lower panel; dotted lines) regarding the transmission of a slab pair structure enclosing several materials with a thickness of 0.5 mm and different dielectric constants, already described in Table 1.
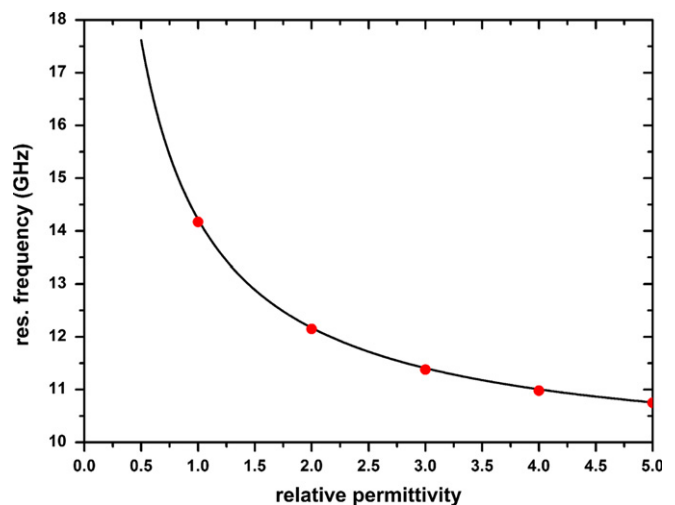
Fig. 3. Magnetic-resonance frequency (f_μ) of the system of paired slabs vs the relative permittivity of the material under sensing (ε_x), calculated using Eq. (4) with $A_1 = 94.00$ GHz^2, and $B_1 = 106.789$ GHz^2 (black line). Red dots correspond to the values of resonance frequency obtained through transmission simulations.
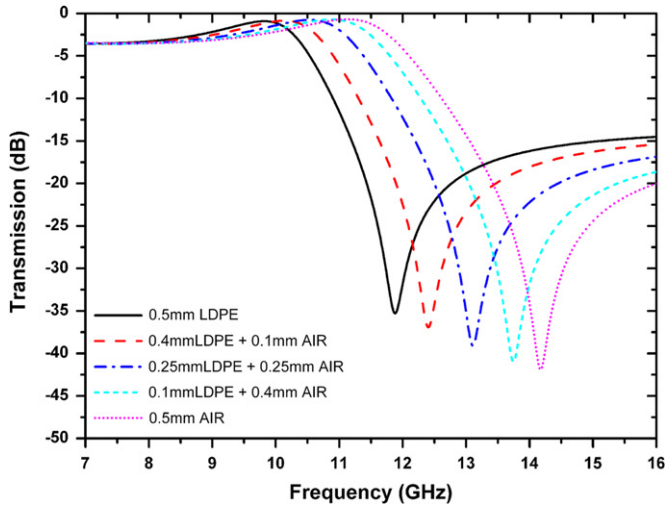
Fig. 4. Simulation results regarding the transmission of a slab pair structure, sensing a LDPE layer of various thicknesses (d_x) placed between the slabs; the rest of the space, of thickness $d-d_x$, is air. The total thickness between the slabs is $d=0.5$ mm.
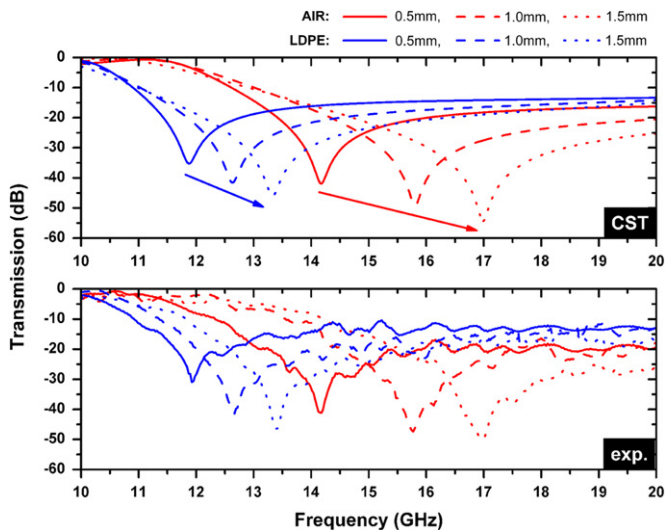
Fig. 5. Simulation results regarding the transmission of a slab pair structure, sensing AIR (red lines) and LDPE (blue lines) of different thicknesses. Here the dielectric material fills all the space between the slabs. (For interpretation of the references to color in this figure legend, the reader is referred to the web version of this article.)

the rest is air. From Fig. 4 one can see that even a very thin layer of LPDE, of thickness $d_x=0.1$ mm, can lead to a resonance frequency shift as large as 0.5 GHz, indicating the large sensitivity of our design.

Fig. 5 illustrates the simulated and the measured transmission for a structure where the thickness of the dielectric material under detection, $d=d_x$, varies between 0.5 mm (as Fig. 2) and 1.5 mm. The dielectric materials here are LDPE and air and they fill all the available space between the slabs. Comparing the resonance frequency difference between the two dielectric materials under detection, we see that this difference, which is $\sim$2.3 GHz for $d=0.5$ mm (solid lines), becomes $\sim$3.7 GHz for $d=d_x=1.5$ mm (dotted lines), showing that the approach becomes even more sensitive if one can provide thicker layers of the material under detection. The dependence of the magnetic resonance frequency on the thickness of the material under detection
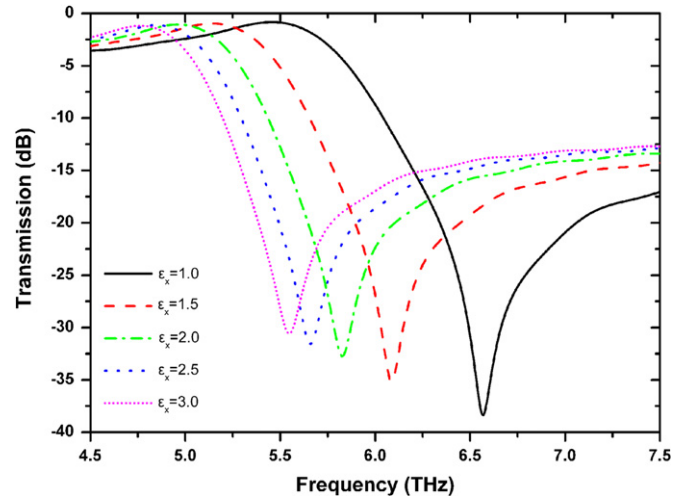
Fig. 6. Simulation results regarding the transmission vs frequency for a slab pair structure sensing dielectrics of permittivity between 1 and 3. The thickness of the dielectric is 0.5 μm, the unit cell of the slab pair has dimensions $a_E a_H = 19$ μm × 19 μm (for the notation see Fig. 1) and the slabs are of size $l=w=14$ μm, with metal thickness 1 μm.

can be qualitatively concluded by Eq. (4) in combination with Eq. (3), as the ε_{eff} of the layered structure between the metallic slabs is reduced if one increases the thickness of the spacer material.

The sensitivity of our sensing approach, especially for dielectrics of low permittivity values, makes it appropriate for operation in THz and IR regimes for the sensing of biomolecular and/or organic materials. This capability of the approach is illustrated in Fig. 6, where we present transmission simulations for a slab-pair system of μm scale, sensing low permittivity dielectrics, of ε between 1 and 3. The pair is now printed on glass substrate ($\varepsilon_b=3.9$) of thickness 1 μm, leaving a space $d=d_x=0.5$ μm between the slabs for the material under detection.

From Fig. 6 one can see that for dielectric materials of ε between 1 and 1.5 there is a magnetic resonance shift, Δf_μ, as large as 0.5 THz, indicating the suitability of our approach for sensing applications in the THz and far-IR regimes. As discussed in the microwave case above, the sensitivity of the design can become even higher if the slabs are printed on Si or GaAs boards. Finally, we have to mention here that slab-pair systems with the dimensions and materials used for Fig. 6 can be easily fabricated using UV lithography and characterized using THz time domain spectroscopy showing signal to noise ratios as high as 1000 (corresponding to −30 dB transmission).

4. Conclusions

We have studied the sensing capability of a metamaterial structure made of pairs of metal slabs, in both microwave and THz regimes. The microwave study has been done by both measuring and simulating the shift of the magnetic resonance frequency as one varies the electrical permittivity and thickness of a dielectric layer placed between the slabs of the pairs. The agreement between measurements and simulations is very good. Our results, showing a larger sensitivity for lower-index dielectrics, can be qualitatively predicted using an LC circuit description of the slab-pair structure. This description can lead also to conditions for increasing the sensitivity of our sensing approach and design. Finally, simulations concerning μm-scale slab-pair-based systems show that our sensing design and approach can be easily applied in the THz regime.

Acknowledgments

References

[1] V.G. Veselago, Sov. Phys. Usp. 10 (1968) 509.
[2] J.B. Pendry, Phys. Rev. Lett. 85 (2000) 3966.
[3] J.B. Pendry, D. Schurig, D.R. Smith, Science 312 (2006) 1780.
[4] N. Engheta, IEEE Antennas Wireless Propag. Lett 1 (2002) 10.
[5] Z. Jakšić, N. Dalarsson, M. Maksimović, Microw. Rev. 12 (2006) 36.
[6] D. Shreiber, M. Cupta, R. Cravey, Sens. Actuat. A 165 (2011) 256.
[7] A.J. Haes, L. Chang, W.L. Klein, R.P. Van Duyne, J. Am. Chem. Soc. 127 (2005) 2264.
[8] A.A. Yanik, M. Huang, A. Artar, T.-Y. Chang, H. Altug, Appl. Phys. Lett. 96 (2010) 021101.
[9] G. Mattei, P. Mazzoldi, M. Post, D. Buso, M. Guglielmi, A. Martucci, Adv. Mater. 19 (2007) 561.
[10] D. Nau, A. Seidel, R.B. Orzekowsky, S.-H. Lee, S. Deb, H. Giessen, Opt. Lett. 35 (2010) 3150.
[11] E.M. Larsson, C. Langhammer, I. Zorić, B. Kasemo, Science 326 (2009) 1091.
[12] J.B. Pendry, A.J. Holden, D.J. Robbins, J.W. Stewart, IEEE Trans. Microwave Theory Tech. 47 (1999) 2075.
[13] J. Zhou, Th. Koschny, M. Kafesaki, E.N. Economou, J.B. Pendry, C.M. Soukoulis, Phys. Rev. Lett. 95 (2005) 223902.
[14] K. Aydin, I. Bulu, K. Guven, M. Kafesaki, C.M. Soukoulis, E. Ozbay, New J. Phys. 7 (2005) 168.
[15] H. Caglayan, S. Cakmakyapan, S.A. Addae, M.A. Pinard, D. Caliskan, K. Aslan, E. Ozbay, Appl. Phys. Lett. 97 (2010) 093701.
[16] I.A. Al-Naib, C. Jansen, M. Koch, App. Phys. Lett. 93 (2008) 083507.
[17] M. Labidi, J.B. Tahar, F. Choubani, Opt. Express 19 (2011) A733.
[18] M. Kafesaki, Th. Koschny, R.S. Penciu, T.F. Gundogdu, E.N. Economou, C.M. Soukoulis, J. Opt. A: Pure Appl. Opt. 7 (2005) S12.
[19] J.F. O'Hara, R. Singh, I. Brener, E. Smirnova, J. Han, A.J. Taylor, W. Zhang, Opt. Express 16 (2008) 1786.
[20] G. Dolling, C. Enkrich, M. Wegener, J.F. Zhou, C.M. Soukoulis, S. Linden, Opt. Lett. 30 (2005) 3198.
[21] R.S. Penciu, M. Kafesaki, Th. Koschny, E.N. Economou, C.M. Soukoulis, Phys. Rev. B 81 (2010) 235111.
[22] J. Zhou, E.N. Economou, Th. Koshny, C.M. Soukoulis, Opt. Lett. 31 (2006) 3620.
[23] I. Bahl, Lumped Elements for RF and Microwave Circuits, Artech House, 2003.